# Chapter 1

# Metrology Applications of Fluid Crystals

## 1.1 Experimental Design

We created freely-suspended smectic films with racetrack geometry, as shown in Fig. 1.1, using 8CB (4-*n*-octylcyanobiphenyl), a fluid smectic A liquid crystal at room temperature that can be drawn into molecularly thin films freely suspended in air [**?**, **?**, **?**]. A mechanical drawing of the film holder is in the Supplemental Information.

Freely-suspended films are ideal flow sensors for several reasons. Because they are so thin, they extract very little energy from the gas jet being measured. A comparison of the effective areal densities in our system assuming mass densities $\rho_{\mathrm{LC}} = 1.008 \times 10^3\,\mathrm{kg/m^3}$ and $\rho_{\mathrm{air}} = 1.225\,\mathrm{kg/m^3}$, and thicknesses 6 nm and 1 cm of the LC film and of the layer of air in the channel respectively, shows that the mass per unit area of the film is about 2000 times smaller than that of the air it is measuring, implying that smectic films should be very sensitive to the velocity of air flowing over them. Smectic films are intrinsically much more stable than films of conventional fluids, lasting up to several years in the laboratory, and have been used previously to probe 2D hydrodynamics [**?**, **?**] and rheology [**?**], shear-stress measurements [**?**], and in pressure metrology [**?**, **?**]. The application

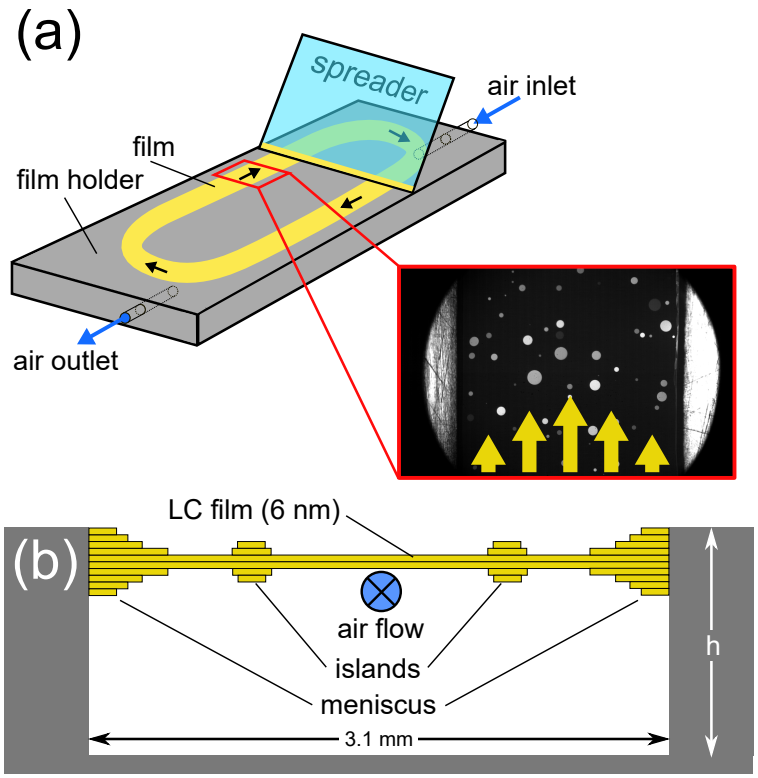


Figure 1.1: Smectic film flow meter geometry. (a) A stainless steel film holder (45.2 mm × 34.8 mm × 7.6 mm) has a $w = 3.1$ mm-wide channel in the form of a racetrack cut to a depth $h = 3.7$ mm. At viewing ports centered along each 'arm', the channel is cut all the way through the film holder (a depth of 7.6 mm). Gas is coupled into and out of the system by means of co-linear, 2 mm-diameter holes at the ends of the film holder. Smectic films are created by coating the bottom of a glass coverslip (the spreader) with liquid crystal material and drawing it across the top opening of the channel. The film is shielded from random air currents from above by a sealed cover (not shown). The photomicrograph shows typical islands (localized regions with more layers than the background film) used to track flow of the film in one of the viewing regions of the racetrack. (b) Schematic cross-section of a smectic film suspended across the channel (not to scale). The film comprises an integer number of smectic layers and can be as thin as two molecules ($\sim$ 6 nm). In general, a meniscus forms where the film contacts the edges of the channel.

described here uses smectic films for flow measurements.

When a film is first drawn, it is typically only a few smectic layers thick and appears uniformly black in reflected light. In the prototype racetrack geometry sketched in Fig. 1.1(a), air is then injected at a known volumetric flow rate into the continuous rectangular channel located beneath the film. The inlet airflow is independently monitored using a mass airflow sensor (Honeywell AWM5101VN) capable of measuring flow rates between 0 and 5 standard litres per minute (SLPM). As the air flows through the channel, it shear couples to the liquid crystal, causing circulation of the film around the racetrack. This flow typically pulls some additional LC material in from the meniscus, leading to the formation of small, disc-like islands embedded in the film. Since the reflectance of thin, freely-suspended films depends quadratically on thickness[**?**], the islands are brighter than the background film and can easily be visualized using video microscopy. The motion of the islands is observed on the "backstretch" of the racetrack using a 5× objective and captured using a high-speed video camera (Vision Research Phantom v12.1) at rates of 100–5000 frames per second. The islands are tracked using the open source Python library Trackpy [**?**], allowing us to use PTV methods [**?**, **?**, **?**, **?**] to measure the velocity field of the film in the region of interest.

The device works by optically measuring the island velocity, which should be linearly coupled to the velocity of the airflow. In contrast to other mechanical flow meters, our flow meter should thus be uniformly sensitive to airflow, regardless of the airflow velocity.

Our experimental approach has much in common with traditional PTV methods, where tracer particles are injected into the gas being measured and a light sheet created by a laser is used to define an illuminated plane, so that the tracer particles intersecting this plane can be tracked with a camera, mapping out the gas flow. A key difference is that our tracer particles (the islands) are embedded in a fluid with low vapor pressure ($< 10^{-6}$ torr)[**?**] that couples hydrodynamically to the gas flow, rather than relying on solid particles introduced into the gas. In the LC flow meter, the gas thus remains free of foreign tracer particles, making this a useful, non-invasive approach for systems where maintaining gas purity is important.

## 1.2 Theory and Simulation

In order to act as an ideal mechanical flow meter, the LC device should couple linearly to the gas flow (i.e., with a sensitivity independent of flow velocity) while having a minimal effect on the system being measured.

Linearity is an intrinsic feature of this system because of the standard no-slip boundary condition between two fluids in contact. Because the velocity of the air varies over the height of the channel, the average air and film velocities will be slightly different.

In order to model the behavior of the LC flow meter, we first consider two-phase, stratified flow in an infinitely long, rectangular pipe with symmetry about the midplane, a geometry that is amenable to an analytic approach [**?**, **?**].

The symmetric rectangular pipe has the essential elements of the racetrack flow meter, a multiphase system where a thin fluid is surrounded by air, but has none of the complicating geometrical factors, allowing us to focus on the intrinsic properties of the air and film interaction. By varying the relative volume of the air and liquid phases (the phase fraction), we can estimate the effect of a fluid with the same thickness as a freely suspended film on the airflow.

We solved the Navier-Stokes equations to determine the airflow in the pipe both with and without the LC film, using appropriate viscosities for the air ($1.8 \times 10^{-5}$ Pa s) and LC film ($5.2 \times 10^{-2}$ Pa s)[**?**]. At values of the phase fraction corresponding to the experiment (with a thick LC film of 60 molecular layers, $\phi \sim 10^{-5}$), the flow of the LC film is found to be coupled identically to that of the air (Fig. 1.2(a)). Furthermore, the air flow in the presence of the LC film is essentially indistinguishable from the flow in the absence of the film (Fig. 1.2(b)), suggesting that, at least in this idealized geometry, the film extracts a negligible amount of energy from the air flow. Details of these calculations are given in the Supplemental Information.

We numerically modeled the flow of air in the 3D racetrack geometry, without the liquid crystal film but choosing track dimensions and flow parameters consistent with our experiments.

Modeling the air flow alone allows us to see the "natural state" of flow in the racetrack

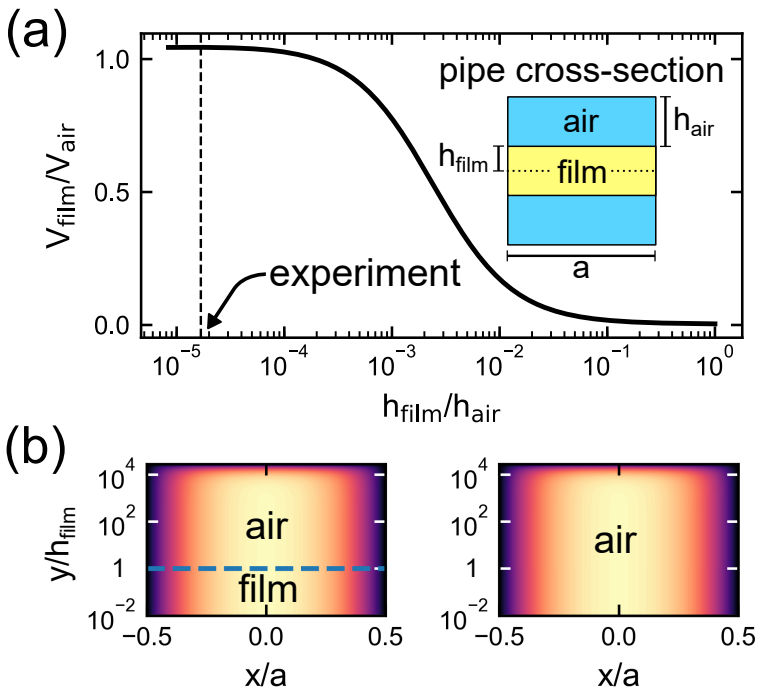


Figure 1.2: Analytic analysis of symmetric, two-phase, stratified fluid flow in an infinitely long pipe of width $a$. (a) Ratio between the average film and air velocities as a function of the phase fraction (the ratio of the volume of the fluid and the volume of the air, $\phi = h_{\text{film}}/h_{\text{air}}$). When the phase fraction is very small, the film is strongly coupled to the air and moves with the same speed. (b) Flow velocity in the top half of the pipe. At left, both air and film are flowing through the pipe (the blue dashed line demarcates the upper boundary of the film), while on the right only air is present. The $y$ dimension is scaled by the half the thickness of the LC film, $h_{\text{film}}$. The flow fields in these two cases are practically indistinguishable, suggesting that the influence of the LC film on the airflow is negligible.

geometry in the absence of the LC film. As the results of the analytical modeling in the previous section suggest that the film has a negligible influence on the airflow, we expect these airflow-only simulations to closely mimic the experimental behaviour.

The results of these simulations then allow us to see whether the geometry of the racetrack modifies the linear sensitivity predicted from the analytical model. We can also test the assumption

that the film has a negligible impact on the overall flow behaviour by comparing the results of the air-flow simulations to the observed experimental flow behaviour.

The simulations were performed using OpenFOAM, an open-source fluid dynamics solver that uses a SIMPLE algorithm[?]. The results are summarized in Fig. 1.3 with further details given in the Supplemental Information. The simulations indicate that at low inlet velocity values ($\lesssim 0.55\,\mathrm{m/s}$) the air stream in the channel splits, so that it flows in the same absolute direction along both arms of the racetrack. At $v_{\mathrm{in}} = 0.55\,\mathrm{m/s}$, the airflow is predicted to transition to homogeneous, clockwise circulation.

The net force on an LC film in contact with the air stream is the sum of the shear forces along the entire length of the racetrack, for which there are two main contributions: the air moving along the shortest distance from the inlet to the outlet (at speed $v_2$), and the air moving along the other side of the racetrack (at speed $v_1$). Because the LC film is incompressible, if $v_1$ and $v_2$ are in the same absolute direction, as in Fig. 1.3(a), then the steady state film velocity is $v_{\mathrm{film}} \propto v_2$-$v_1$. This predicted film speed is in general lower than but roughly proportional to the inlet air flow, as shown in Fig. 1.3(b).

We think that the chaotic flow we observe in the racetrack is a manifestation of the 'split-flow' predicted by the simulations. We hypothesize that the film acts to bias the air-film system to a circulating regime, explaining why the air-film onset to circulating flow happens at lower inlet velocities than the simulations predict for pure airflow.

In summary, the analytic and numerical models both suggest that freely-suspended LC films in racetrack geometry should make excellent flow detectors, linearly coupling to and stabilizing the air flow.

## 1.3 Results and Discussion

We measured the velocity fields of LC films coupled to inlet airflows in the range 0.1 SLPM–0.4 SLPM. We observed three main regimes of film flow behaviour, indicated by the shading in Fig. 1.3(c). Below a threshold inlet air velocity ($v_{\mathrm{in}} < 0.3\,\mathrm{m/s}$), the flow is characterized by time-

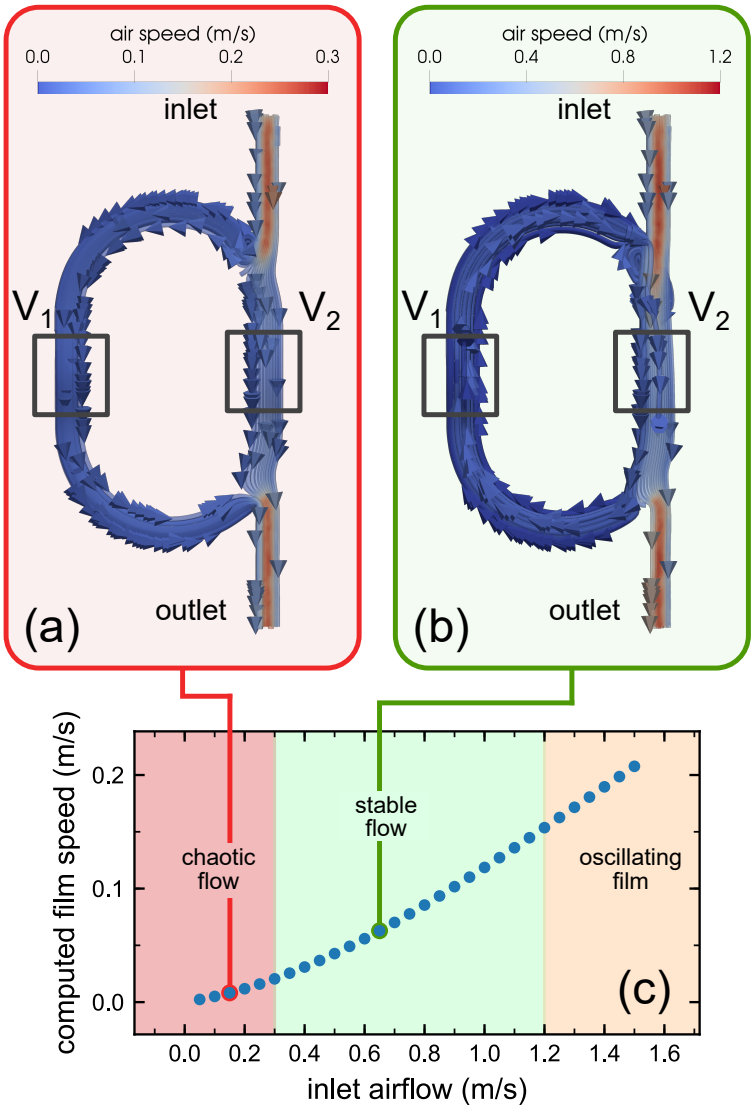


Figure 1.3: Computed airflow in the racetrack geometry. (a) Model velocity field for inlet velocity $v_{\text{inlet}} = 0.15\,\text{m/s}$. The air does not circulate uniformly in the same sense around the racetrack, instead splitting between the front and back legs. (b) Model velocity field for inlet velocity $v_{\text{inlet}} = 0.65\,\text{m/s}$. Above a transition inlet velocity of $v_{\text{inlet}} = 0.55\,\text{m/s}$, the air circulates uniformly around the racetrack. (c) Predicted net film speed ($v_{\text{film}} \propto v_2 - v_1$) for a range of inlet velocities. The slope of this curve gives an average theoretical sensitivity of $S = 0.15$. The background shading reflects the experimental observations with different inlet velocities: for $v_{\text{in}} < 0.3\,\text{m/s}$, the film flow is chaotic; for $0.3\,\text{m/s} < v_{\text{in}} < 1.2\,\text{m/s}$, the film exhibits stable Poiseuille flow; for $v_{\text{in}} > 1.2\,\text{m/s}$, the film undergoes rapid out-of-plane oscillations that make particle tracking impractical.

dependent, chaotic behavior, with flow reversal and eddy currents observed in the films. This behavior is likely due to flow splitting of the type shown in Fig. 1.3(a), where the incoming air stream is divided between the short and long arms of the racetrack.

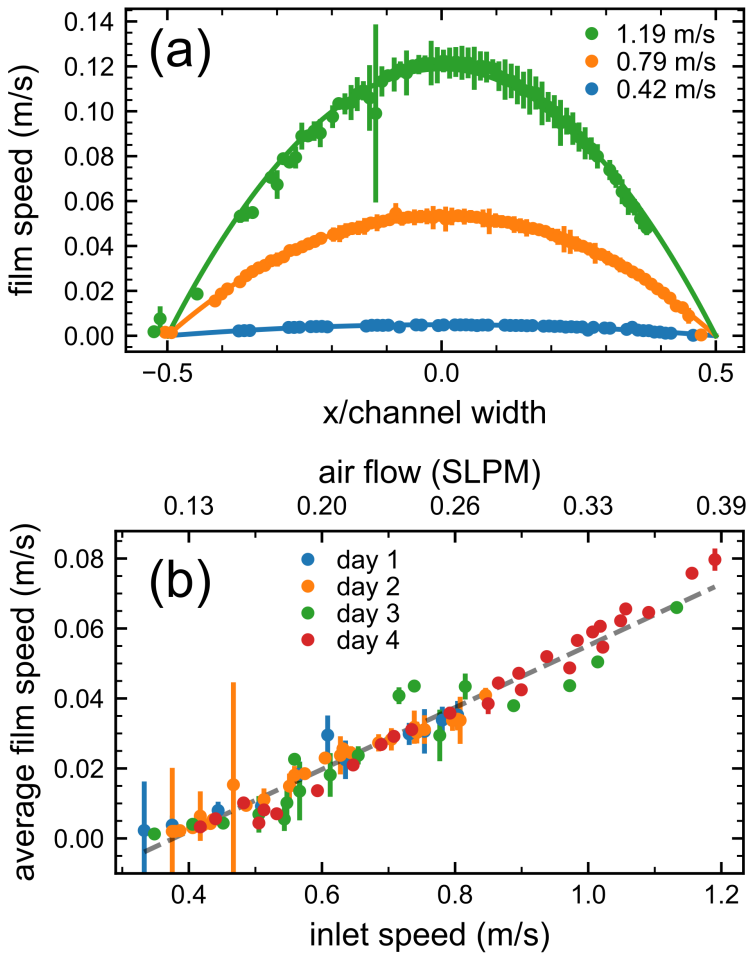


Figure 1.4: Characterization of flow meter. (a) Velocity profiles over the width of the racetrack channel, with each point corresponding to a specific tracked island. The profiles are well described by parabolas (smooth curves), confirming Poiseuille flow over a wide-range of inlet velocities. At higher velocities, the data are noisier due to the relatively paucity of islands that can be captured in sequential frames. The left-right asymmetry in the number of measurements is an artifact due to defects on one side of the camera sensor. (b) Spatially averaged film velocity in the observation region as a function of inlet air velocity. Measurements were performed over four separate days, using more than 30 films. The volumetric flow rate of the air being injected into the racetrack through the inlet was measured using an independent mechanical sensor. The average film speed is linearly proportional to the speed of the air at the device inlet, with a sensitivity that is independent of flow rate.

At intermediate air inlet velocities ($0.3\,\mathrm{m/s} < v_{\mathrm{in}} < 1.2\,\mathrm{m/s}$), the film undergoes uniform, counter-clockwise circulation around the racetrack, as shown in Fig. 1.4(a), with a Poiseuille flow profile across the film that stabilizes in less than 1 second. The observed threshold speed for the transition from chaotic flow to uniform circulation ($v_{\mathrm{in}} \sim 0.3\,\mathrm{m/s}$) is somewhat lower than predicted by the simulations for airflow alone ($v_{\mathrm{in}} \sim 0.55\,\mathrm{m/s}$). This suggests that the film acts to stabilize homogeneous flow, promoting a uniform, regular circulation of the film and air. Because our measurement relies on obtaining regular, simple flow, the stable regime is clearly optimal for operation of the flow meter, and extending the usable range to lower inlet velocities is a clear advantage of the LC film-air system. At high air inlet velocities ($v_{\mathrm{in}} > 1.2\,\mathrm{m/s}$), the film oscillates rapidly up and down, causing the islands to go in and out of focus and the film eventually to break.

A comparison of the spatially averaged film speed measured half way along the back stretch of the racetrack to the independently measured inlet airflow is plotted in Fig. 1.4(b). The average slope of this graph gives a measured sensitivity of the flow meter of $S = 0.09$. This is slightly less than the sensitivity predicted from the pure airflow simulations, a difference which we attribute to air loss during the air-injection process. With some refinement of the racetrack geometry, we would expect to extend the accessible measurement range to lower velocities. The upper velocity limit could be raised by implementing measures to equalize the air pressure across the film. We believe that such differences in air pressure are responsible for the rapid vertical oscillations observed at high flow rates.

By harnessing the unique properties of freely-suspended smectic films, we have demonstrated a method for mechanical measurement of air flow that has intrinsically linear sensitivity. This technique could usefully be applied to mapping the velocity field of gases flowing through exotic microfluidic geometries in two dimensions.